UNLV | UNIVERSITY LIBRARIES

Electrical and Computer Engineering Faculty Publications

Electrical & Computer Engineering

3-1997

Theoretical Study of a Linear Accelerator Used As a VUV/X-ray Source Using the Inverse Compton Scattering Mechanism: Comparisons and Applications

Robert A. Schill Jr.
University of Nevada, Las Vegas, robert.schill@unlv.edu

Edward McCrea
EG&G Energy Measurements

Follow this and additional works at: https://digitalscholarship.unlv.edu/ece_fac_articles

Part of the Computer Engineering Commons, and the Electrical and Computer Engineering Commons

Repository Citation

Schill, R. A., McCrea, E. (1997). Theoretical Study of a Linear Accelerator Used As a VUV/X-ray Source Using the Inverse Compton Scattering Mechanism: Comparisons and Applications. *Laser and Particle Beams, 15*(1), 179-196.
https://digitalscholarship.unlv.edu/ece_fac_articles/579

This Article is protected by copyright and/or related rights. It has been brought to you by Digital Scholarship@UNLV with permission from the rights-holder(s). You are free to use this Article in any way that is permitted by the copyright and related rights legislation that applies to your use. For other uses you need to obtain permission from the rights-holder(s) directly, unless additional rights are indicated by a Creative Commons license in the record and/or on the work itself.

This Article has been accepted for inclusion in Electrical and Computer Engineering Faculty Publications by an authorized administrator of Digital Scholarship@UNLV. For more information, please contact digitalscholarship@unlv.edu.

Laser and Particle Beams (1997), *vol.* 15, *no.* 1, *pp.* 179–196
Printed in the United States of America

Theoretical study of a linear accelerator used as a VUV/X-ray source using the inverse Compton scattering mechanism: Comparisons and applications

By ROBERT A. SCHILL, JR.* AND EDWARD McCREA**
*Electrical and Computer Engineering, University of Nevada Las Vegas, 4505 Maryland Parkway, Las Vegas, Nevada 89154-4026
**EG&G Energy Measurements, Las Vegas Area Operations, P.O. Box 1912, Las Vegas, Nevada 89125

(Received 4 October 1995; Revised 4 June 1996; Accepted 9 June 1996)

A classical linear theory is used to compare large synchrotron sources to a rf linear accelerator employed as a VUV/X-ray source. Comparisons are made on a per-pulse basis. It is demonstrated that the linear accelerator as an X-ray source is comparable to large synchrotron accelerators with wiggler insertion devices at the experiment. Applications to lithography, X-ray microscopy, X-ray spectroscopy and detector calibration are examined. Excluding lithography, the linear accelerator with an appropriate laser source is a useful source of X rays for these applications. As verification, classical results are compared with quantum mechanical results and are shown to be in good agreement.

1. Introduction

Over 700 low-energy and medium-energy (0.12- to 16-MeV) electron sources have found a market in the industrial (Silverman 1995) and medical sectors. The use of such accelerators for a wide range of environmental problems including the treatment of sewage sludge and waste water, the removal of NO_x and SO_x from flue gases, and the sterilization of biomedical supplies (Silverman 1995) will warrant the increased usage of such sources. In some applications, pulse sources are more efficient than continuous sources. Modifying the electron source to be a light source as well will open up opportunities for multiple applications.

Recently, a proof of principle experiment on a Laser Synchrotron Source (Ting *et al.* 1995) configuration was performed using a Naval Research Laboratory (NRL) tabletop 1 to 2 J, 1.18 eV (1.053 μm), terawatt laser and the NRL 0.6- to 1-MeV, 55-ns pulsed Febetron accelerator. X-ray photon energies of 20 eV were measured. It was estimated that about 1×10^6 photons were generated. Due to the convergence of the electron beam, these photons exited the source in approximately a 40° half angle. Theory and experimentation indicate that 550 of these photons were detected by a 1 cm^2 detector about 35 cm from the interaction region. This appears to be the first observation of X rays in the tens of eV range generated by Thomson scattering of near infrared photons from a relativistic electron beam.

A different study (Sprangle *et al.* 1989) has shown that $\frac{1}{4}$-GW, 1.2-mm microwaves scattered from $\frac{1}{4}$- to $\frac{1}{2}$-GeV electrons can produce enough X-ray photons useful for X-ray lithography. A quasi-optical gyrotron would be a source for the microwaves and the electron beam would be supported by a storage ring. Due to the size, weight and expense, it may not be economically practical for industry to own such a source for research or commercial purposes.

© 1997 Cambridge University Press 0263-0346/97 $11.00 + .10

It is the intent of this paper to examine the practical application of a medium energy (1-MeV to 50-MeV), pulsed, linear accelerator and compare its capability to generate intense UV/X-ray light with existing non-nuclear sources. The linear inverse Compton scattering mechanism is employed. Back of the envelope calculations indicate that such a source is appropriate in the fields of X-ray microscopy, X-ray spectroscopy, and detector calibration. Unless very sensitive photo-resists exist or very high repetition rates are achieved, such a source does not appear to be very practical in X-ray lithography. Due to the energy tunability of this source and its highly focused intense beam, this source may find application as a tool for internal and external surgery in the medical field. Researchers at the Vanderbilt Medical Free Electron Laser Facility are focusing their efforts on various medical applications, including: wound healing, modulation of protein, synthesis, melting of DNA and RNA, diagnosis and treating of breast cancer, therapeutic uses, and airway and brain surgery (Carroll 1991a,b, 1994; Carroll *et al.* 1994). Brightness and flux comparisons are also made with relatively new synchrotron sources; the Advanced Light Source at Berkeley (ALS) and the Advance Photon Source (APS) at Argonne National Laboratory. Some of the technical and practical aspects are examined.

A self-consistent classical linear theory is used to examine the scattering of pulsed infrared and optical photon beams from a pulsed relativistic electron beam. The method is based on the Lienard–Wiechert potentials. Both the laser beam and the electron beam are assumed to be cylindrical with a Gaussian profile. The beams are antiparallel and collide head-on. Esarey *et al.* (1993) developed a set of expressions characterizing nonlinear Thomson scattering of intense laser pulses from beams and plasmas. For the applications considered, the normalized laser strength parameter is much less than one. Therefore, only the linear scattering problem is of concern. In this limit, their differential spectral energy per differential solid angle is employed. A different work (Schill 1996) has obtained in a self-consistent manner the total powers and total differential powers per solid angle. These relations are also employed. It is assumed that the frequency width of the radiation spectrum is sharply peaked about the resonant frequency. For appreciable scattered power, it is crucial that the beams be highly focused.

These calculations are verified using a quantum mechanical model based on standard cross-section methods employing the Klein–Nishina formula. The cylindrical beams are assumed to have a uniform density profile transverse to the direction of motion. Beyond the beam radius, the appropriate photon or electron density is zero. In all cases examined, the quantum mechanical results are a factor of about 4.25 larger than the classical results. This is reasonable because about 63% of the photons and electrons in the uniform density profiles exist within the respective laser and electron beam waists in the classical model.

This paper is organized in the following fashion. Section 2 yields the governing relations for the classical and quantum mechanical models. Comparisons are made between the classical and the quantum mechanical models in section 3. Observations are presented and, due to linearity, a scaling law is identified. Section 4 compares synchrotron accelerators with insertion devices used as an X-ray source with the linear accelerator employing inverse Compton scattering generating the same radiation. Applications are identified in section 5. Section 6 concludes the paper.

2. Governing relations for the classical and quantum mechanical models

A Gaussian electron beam with drift velocity $v_o\hat{z}$, beam waist W_{eb}, and number density N_o collides head-on with an $\hat{x}$ linearly polarized, Gaussian, laser beam propagating in the $-v_o\hat{z}$ direction with a beam waist W_o, a source angular frequency ω_s, and an electric field amplitude E_o. In the region of interaction, the laser beam is focused to its waist. The

pulse duration of both beams is small yielding a small length of overlap L_o. Consequently, the phase front of the laser beam approximates a plane wave front throughout this region. A linear scattering process is of interest, therefore, the normalized laser strength parameter a_o [$=(qE_o/m_oc\omega_s)$ or (qA_o/m_oc) in MKS units; $=(qA_o/m_oc^2)$ in CGS units] is much less than one. In this limit, the differential spectral energy per differential solid angle obtained by others (Esarey *et al.* 1993) can be simplified to yield

$$\frac{dW(\hat{r},\omega)}{d\Omega} = \sum_{f=-\infty}^{\infty} \frac{q^2f^2\omega_d^2}{4\pi\varepsilon_o c}\left[\left(\frac{1-\cos^2\phi_o\sin^2\theta_o}{\sin^2\theta_o\cos^2\phi_o}\right) + \beta_o\frac{(\beta_o-\cos\theta_o)}{(1-\beta_o\cos\theta_o)^2} - \frac{\beta_o\cos\theta_o}{(1-\beta_o\cos\theta_o)}\right] \times J_f^2(\tilde{\Delta})\delta^2(\omega(1-\beta_o\cos\theta_o)-f\omega_d), \tag{1}$$

where

$$\tilde{\Delta} = -\Delta e^{-(x_o^2+y_o^2)/W_o^2} \tag{2}$$

$$\Delta = \frac{fa_o}{\gamma_o}\frac{\sin\theta_o\cos\phi_o}{(1-\beta_o\cos\theta_o)} \tag{3}$$

$$\omega_d = \omega_s(1+\beta_o) \tag{4}$$

$$\tilde{V}(\theta_o,\phi_o) = \frac{1}{[1-\beta_o\cos\theta_o]}\left[\beta_o\frac{[\beta_o-\cos\theta_o]}{[1-\beta_o\cos\theta_o]^2} - \frac{\beta_o\cos\theta_o}{[1-\beta_o\cos\theta_o]} + \frac{1-\cos^2\phi_o\sin^2\theta_o}{\cos^2\phi_o\sin^2\theta_o}\right]. \tag{5}$$

The phase terms are omitted because this information is lost in the power calculation. Further, the frequency width of the radiation spectrum is assumed to be sharply peaked about the resonant frequency.

The total differential power scattered per solid angle and the total power scattered between $\theta_{o_{\min}}$ and $\theta_{o_{\max}}$ both due to all electron scatterers obtained from equation (1) are, respectively (Schill 1996),

$$\frac{dP_T}{d\Omega} \approx \sum_{f=1}^{\infty}\frac{q^2f^2\omega_d^2L_oN_o}{8\pi\varepsilon_o c}\frac{W_{eb}^2W_o^2}{2fW_{eb}^2+W_o^2}J_f^2(\Delta)\tilde{V}(\theta_o,\phi_o) \tag{6}$$

$$P_T \approx \sum_{f=1}^{\infty}\frac{q^2f^2\omega_d^2L_oN_o}{8\pi\varepsilon_o c}\frac{W_{eb}^2W_o^2}{2fW_{eb}^2+W_o^2}J_f^2\left(\frac{fa_o}{\gamma_o}\right)[\beta_o^2S_{f00}^a-\beta_oS_{f00}^b+S_{f00}^c-S_{f00}^d], \tag{7}$$

where

$$S_{f00}^a = 2\pi\left[\prod_{b=1}^{f}\frac{(2b-1)}{2b}\right]\left[\int_{x_{\min}}^{x_{\max}}\frac{(1-x^2)^f}{(1-\beta_ox)^{2f+3}} - dx\frac{c}{v_o}\int_{x_{\min}}^{x_{\max}}\frac{x(1-x^2)^f}{(1-\beta_ox)^{2f+3}}dx\right] \tag{8}$$

$$S_{f00}^b = 2\pi\left[\prod_{b=1}^{f}\frac{(2b-1)}{2b}\right]\int_{x_{\min}}^{x_{\max}}\frac{x(1-x^2)^f}{(1-\beta_ox)^{2f+2}}dx \tag{9}$$

$$S_{f00}^c = 2\pi\int_{x_{\min}}^{x_{\max}}\frac{(1-x^2)^{f-1}}{(1-\beta_ox)^{2f+1}}dx \tag{10}$$

$$S_{f00}^d = 2\pi\left[\prod_{b=1}^{f}\frac{(2b-1)}{2b}\right]\int_{x_{\min}}^{x_{\max}}\frac{(1-x^2)^f}{(1-\beta_ox)^{2f+1}}dx \tag{11}$$

The limits of integration are given as

$$x_{\max} = \cos\theta_{o_{\min}} \tag{12}$$

$$x_{\min} = \cos\theta_{o_{\max}} \ . \tag{13}$$

The half bandwidth resolution on both sides of the center frequency of the scattered radiation ω located at an angle θ_o from the backscattered direction are

$$\theta_{o_{\substack{\min\\ \max}}} = \cos^{-1}\left[\frac{\beta_o\cos\theta_o \pm \dfrac{\Delta\omega}{2\omega}}{\beta_o\left(1 \pm \dfrac{\Delta\omega}{2\omega}\right)}\right], \tag{14}$$

where

$$\theta_o = \cos^{-1}\left[\frac{1}{\beta_o}\left\{1 - f(1+\beta_o)\left(\frac{\omega_s}{\omega}\right)\right\}\right]. \tag{15}$$

For a laser beam of frequency ω_s, the scattered radiation of center frequency ω and full bandwidth $\Delta\omega$ subtends the angle $\theta_{o_{\max}} - \theta_{o_{\min}}$ about θ_o. In the special case when the scattered frequency of radiation is the maximum frequency generated ($\theta_o = 0$), the full bandwidth radiation subtends the angle $0 < \theta_o < 2\theta_{o_{\max}}$. Once a bandwidth is specified, the angle in which the radiation subtends is fixed.

Conservation of energy and momentum in elastic collisions dictate the interaction between an electron and a photon. It is well known that the scalar product of the four vector momentum is invariant under a Lorentz transformation. Employing this, others have determined the scattered photon energy as a function of the incident photon energy, the incident electron energy, and the angular dependence of the trajectories among the incident photon, scattered photon and the electron (Jauch & Rotrlich 1955). Assume a pulsed photon beam impinges head-on with a stationary target of cross sectional area A_e and thickness h_e. Let $\mathcal{N}_e$ be the total number of electrons in a cylindrical electron beam pulse of volume V_e. Assume that the photons are uniformly distributed throughout the cylindrical beam of cross section A_p and length h_p. It can be shown that the total energy scattered into solid angle due to incident photons impinging on the target electrons in a cross-sectional area A is

$$\frac{dE}{d\Omega}\,\Delta\Omega = \hbar\omega\,\frac{d\sigma}{d\Omega}\left(\frac{\mathcal{N}_e\mathcal{N}_p}{A_eA_p}\right)A\Delta\Omega, \tag{16}$$

where A is equal to the smaller of the two beam cross-sectional areas either A_e or A_p. The differential cross-section per unit solid angle for Compton scattering is characterized by the Klein–Nishina formula (Jauch & Rotrlich 1955). The power scattered into solid angle is obtained by dividing equation (16) by the pulse duration in the laboratory frame (detector frame) of reference. Classical mechanics dictates that the scattered wave pulse duration as observed by the detector is

$$\Delta t = \frac{(1-\beta)\tau_p + 2\beta\tau_e}{1+\beta}, \tag{17}$$

where τ_p and τ_e are, respectively, the pulse duration of the incident photon and the electron beam in the laboratory frame. Consequently, the differential power scattered per unit solid angle is

$$\frac{dP}{d\Omega}\,\Delta\Omega = \frac{\hbar\omega}{\Delta t}\,\frac{d\sigma}{d\Omega}\left(\frac{\mathcal{N}_e\mathcal{N}_p}{A_eA_p}\right)A\Delta\Omega. \tag{18}$$

The synchrotron accelerator community measures the performance of their accelerators by the flux of photons generated and the brightness or brilliance of the generated beam in a specified bandwidth. For completeness, an expression for the scattered photon flux and brilliance is provided. Let T correspond to the emission time that is a finite time duration. Incorporating all electron scatterers in the Gaussian electron beam and integrating over solid angle, the total power radiated in any range of conical angle is effectively,

$$W_T = TP_T. \tag{19}$$

With the aid of equations (7)–(15) and (19), the total number of photons generated with a center angular frequency ω in a narrow spectral full bandwidth $\Delta\omega$ is given by

$$N_{p\text{scattered}}(\omega) = \frac{W_T(\omega, \Delta\omega)}{\hbar\omega}, \tag{20}$$

where the full bandwidth $\Delta\omega$ corresponds directly to a spread in conical angle $\Delta\theta$.

Brilliance is typically defined as the amount of differential power scattered per differential solid angle resulting from a differential cross section of overlap between the incident photons and the electron beam. The expression for brilliance is given as

$$B(\Omega, A_s) = \frac{d^2P_T}{d\Omega dA_s}. \tag{21}$$

Equation (6) represents the total differential power scattered per differential solid angle due to the interaction of all the photons and electrons in the region of overlap. It can be deduced from a different work (Schill 1996), that the power scattered per solid angle due to those electrons and photons in the differential area dA_s in the interaction region is equivalent to equation (6) if

$$\frac{\pi W_{eb}^2 W_o^2}{2fW_{eb}^2 + W_o^2} J_f^2(\Delta)$$

is replaced by

$$(\Delta/2)\exp\left[-(x_o^2 + y_o^2)\left(\frac{2f}{W_o^2} + \frac{1}{W_{eb}^2}\right)\right] dA_s.$$

It is common in the synchrotron community to specify the brilliance or brightness in a percent bandwidth. Because the operating frequency is angle dependent, placing a constraint on the bandwidth automatically constrains the angle of radiation in the brilliance. Consequently, when determining the brilliance, the power per area of overlap in cross section within a percent bandwidth tolerance is determined in the time domain and then divided by the solid angle in which the scattered radiation subtends.

3. Scaling, observations, and theoretical comparisons

Observations and theoretical comparisons are made at a monochromatic electron beam energy. For brevity, it is assumed that the electron beam energy is 25 MeV. All relative comparisons appear to be independent of electron beam energy. In this section the aperture opening is either a pinhole or an annular ring. The dimension of the opening is determined by the element of conical angle about a central conical angle relative to the direction of motion of the electron beam with origin in the interaction region (figure 1). Therefore, excluding the $\theta_o = 0$ center angle, the geometrical structure of the beam of radiation is an annular cone. Total power, brilliance, photon flux, and resolutions are examined.

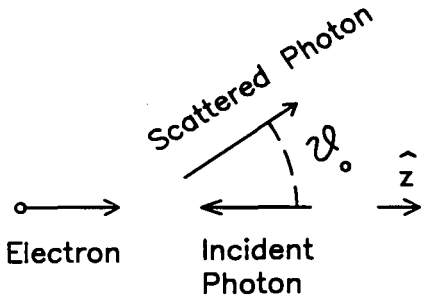

FIGURE 1. The geometry of the scattering process for the classical model. Note, θ_o is the angle the scattered photon makes with the original direction of the electron beam. The backscattered direction is $\theta_o = 0$.

A useful scaling can be observed from equations (1), (6), (7), (20), and (21). Due to linearity, the power, power scattered per solid angle, total scattered energy, flux, brilliance, and number of photons are directly proportional to the laser beam energy and the electron number. Consequently, increasing or decreasing the laser beam energy (keeping the photon energy constant) or the electron number by an order of magnitude increases or decreases by the same order of magnitude the scattered power, flux, brilliance, number of photons scattered, differential power scattered per solid angle, and the total scattered energy. Such a scaling can be directly applied to this and the remaining sections of this paper.

Figure 2 shows that a CO_2 photon colliding head-on with a 25-MeV electron will scatter photons between 0.975 and 1.170 keV within a 0.05° angle from the original direction of motion of the electron beam (figure 1). The 1-J, 1-mm waist, 5-ns pulsed Gaussian beam interacts with the 5-nC, 1-mm waist, 50-ps pulsed Gaussian electron beam in an interaction

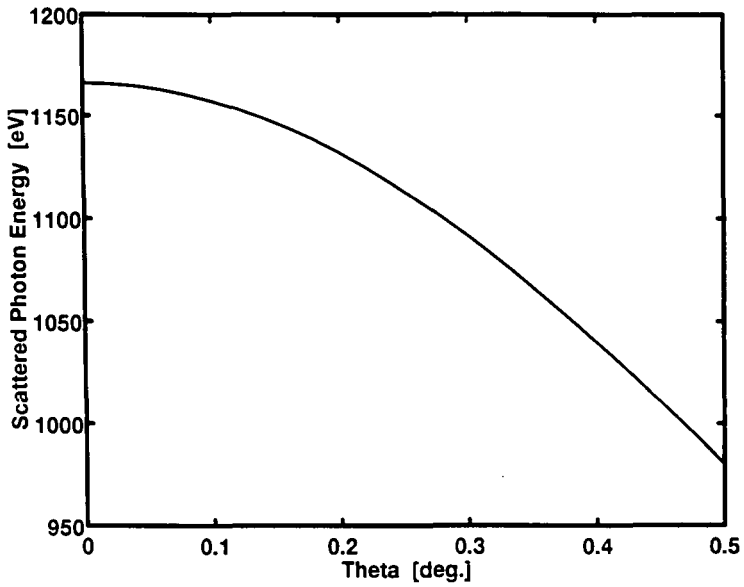

FIGURE 2. The energy of the scattered photon as a result of a CO_2 photon colliding head-on with a 25-MeV electron. The classical and quantum mechanical models agree almost exactly.

region of about 0.75 m in length. Beyond a couple of degrees from the backscattered direction, the power and flux decrease rapidly resulting in a narrow beamwidth. Figures 3a to 3c exhibit the total power, flux, and brilliance in 0.05° conical angle increments about a center angle either shown on the abscissa or deduced with the aid of figure 2. Figure 3d yields the resolution of the beam. It is noted that the energy and the resolution plots, figures 2 and 3d, agree exactly with the quantum mechanical model. Resolution and practicality dictate that the useful portion of the beam occurs at the maximum energy or backscattered direction ($\theta_o = 0$). In the backscattered direction ($\theta_o = 0$), the power, flux, and brilliance are, respectively, about 0.45 W, 0.2×10^{16} photons/s in a 50.5-ps pulse, and 8.4×10^{20} photons/s/sr/mm^2. Within a factor of about 4.25, both quantum mechanical and classical models yield the same result as shown in figures 3a–c. This is justified because the classical theory assumes that the beams are Gaussian in nature whereas the quantum model assumes cylindrical beams of uniform density. Consequently, the quantum model contains about 1.5 times more electrons and 1.5 times more photons as compared to the classical model in a 1-mm waist. Therefore, the classical and quantum models are in good agreement.

4. Comparisons among synchrotron accelerators

Comparisons will be made based on the photon flux and the brilliance as generated on a per-pulse basis. The two synchrotron sources, which the linear accelerator as a light source is to be compared with, are the ALS in Berkeley, CA and the APS at Argonne National Laboratory.

Between about 0.5 and 2.5 keV, the ALS flux from wigglers is approximately 2.5×10^{15} photons per second in a 0.1% bandwidth (Lawrence Berkeley Laboratory Report 1994). This assumes a horizontal aperture of about ±2.5 mrad, an electron beam energy of 1.5 GeV, and a 400-mA current. Increasing the energy to about 20 keV, the flux decreases over two orders of magnitude. The APS accelerators maintain an average photon flux from wigglers (Shenoy *et al.* 1988; Lai *et al.* 1993) of about 3×10^{14} photons per second in a 0.1% bandwidth per mrad in an energy range between 0.1 and 100 keV. Both the APS-A and APS-B machines accelerate the electrons to about 7 GeV with a current capacity of about 100 mA. The former machine has an aperture opening of about 2 mrad with a flux of 2.24×10^{14} photons per second per mrad at the critical energy while that of the latter machine has a 1-mrad aperture with a flux of 4.48×10^{14} photons per second per mrad at the critical energy. The maximum flux averages about 4.5×10^{14} photons per second in a 0.1% bandwidth for both machines.

The circumference of the ALS is 196.8 m. In nominal operation (Lawrence Berkeley Laboratory Report 1989), the accelerator supports 250 buckets where each bucket is filled with a bunch current of 1.6 mA. Each bunch has a full width at half maximum of 35 ps. The orbital period is 656 ns. The number of bunches that radiate per second is 3.81×10^8 s^{-1}. Consequently, the number of photons with energies between 500 eV and 2.5 keV generated per bunch or pulse is approximately 6.56×10^6 photons in a 0.1% bandwidth. It must be understood that this is the estimated number of photons generated inside the storage ring and not at the experiment. Knowing the time of flight of the bunch along a wiggler the power generated may be determined. A typical 16-cm wiggler will interact with the bunch during a time duration of 0.533 ns. Therefore, a 2-keV photon bunch will generate 3.94 W.

The circumference of the APS storage ring is 1060 m. In nominal operation (Shenoy *et al.* 1988), the accelerator supports a maximum of 1248 buckets. Typical number of bunches is from 1 to 60 with a single bunch current of 5 mA. The bunch width is 119 ps. The orbital period is 3.536 μs. A beam current of 100 mA implies that the APS storage ring supports 20 bunches. Consequently, the number of bunches per second that radiate

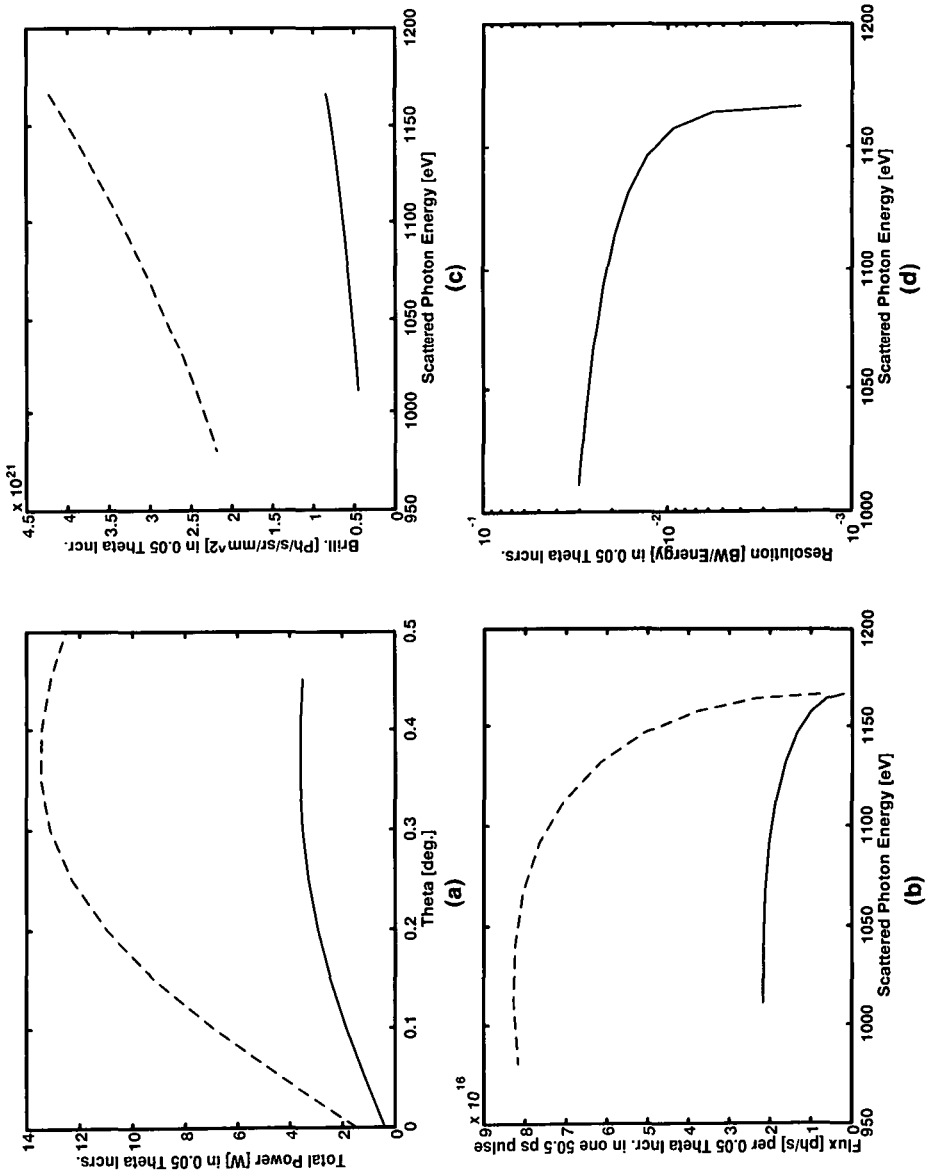

FIGURE 3. A 1-J, 1-mm waist, 5-ns pulsed, Gaussian CO_2 laser beam collides head-on with a 5-nC, 1-mm waist, 50-ps pulsed, 25-MeV electron beam. The (a) total power, (b) flux, (c) brilliance, and (d) resolution of the scattered radiation is exhibited for both the classical (solid line) and the quantum mechanical (dashed line) models. The two theories differ by a factor of about 4.25 or less. A 0.05^0 conical angle element about a central angle was used. The central angle is deduced from the abscissa with the aid of figure 2.

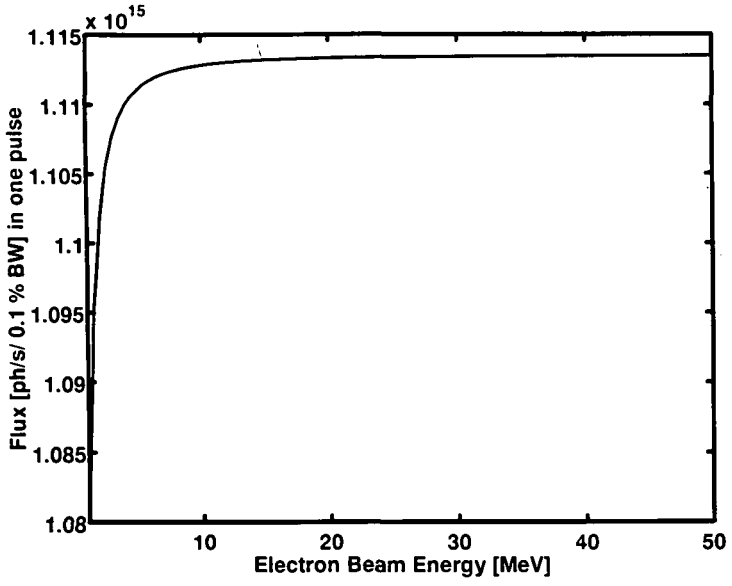

FIGURE 4. A 1-J, 5-ns pulsed, 1-mm waist, Gaussian CO_2 laser beam collides head-on with a 5-nC, 50-ps pulsed, 1-mm waist Gaussian electron beam with energies ranging between 1 and 50 MeV. The flux of photons in one pulse is depicted. For electron beam energies greater than about 5 MeV, the flux in a 0.1% bandwidth is relatively constant. The backscattered photon energies can be determined with the aid of figure 5.

is 5.66×10^6 s^{-1}. As a result, the number of photons with energies between 0.1 and 100 keV generated per bunch or pulse is approximately 8×10^7 photons in a 0.1% bandwidth. As above, this is the estimated number of photons generated inside the machine and not at the experiment. One can easily obtain the power generated by knowing the time of flight of the bunch along a wiggler. A typical 1.5- to 5-m wiggler will interact with a bunch in a time duration of 5 to 16.7 ns, respectively.

Figure 4 illustrates the scattered photon flux generated by the linear accelerator when a 5-nC, 50-ps electron beam collides head-on with a 1-J, 5-ns CO_2 laser. The electron beam energies range between 1 and 50 MeV, generating backscattered photons approximately between 0.1 and 4.5 keV (figure 5). Both beams are focused to have a 1-mm beam waist. Better than 1.1×10^{15} photons per second in a 0.1% bandwidth are generated in a single pulse for electron beam energies greater than 5 MeV. As shown in figure 6, the pulse duration is between 50 and 60 ps. From figure 7, it is observed that about 6×10^4 photons in a 0.1% bandwidth are generated per pulse in this energy range. Figure 8 shows that the conical angle of radiation increases rapidly at the lower beam energies if the bandwidth is constrained to be 0.1%. Because the total number of photons increases as the beam energy decreases (figure 7), a more selective bandwidth can be achieved by decreasing the aperture opening.

Figure 9 illustrates the scattered photon flux generated by the linear accelerator when a 5-nC, 50-ps electron beam collides head-on with a 1-J, 5-ns ruby laser. The electron beam energies range between 1 to 50 MeV, generating backscattered photons approximately between 1 to 70 keV (figure 10). Both beams are focused to have a 1-mm beam waist. Better than 7.25×10^{13} photons per second in a 0.1% bandwidth are generated in a single pulse for electron beam energies greater than 5 MeV. As shown in figure 11, the pulse duration is between 50 and 60 ps. From figure 12, it is observed that about 3.75×10^3 photons

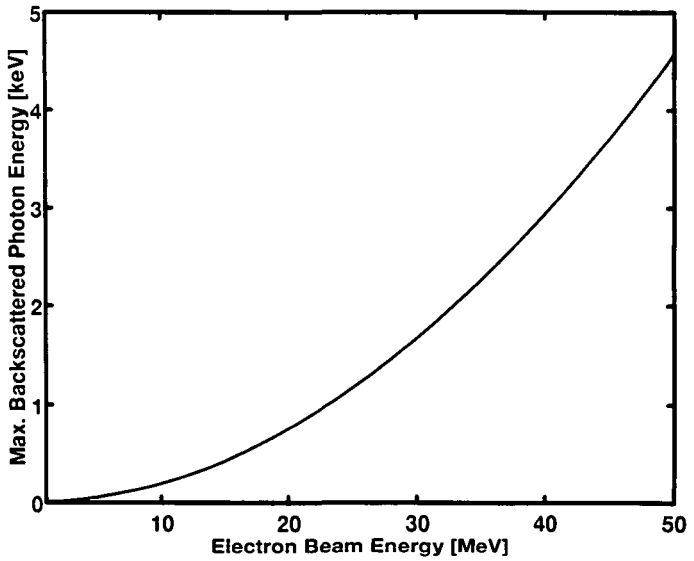

FIGURE 5. The backscattered photon energy ($\theta_o = 0$) resulting from a CO_2 photon colliding head-on with an electron accelerated to energies between 1 and 50 MeV. Energies between .1 and 4.5 keV may be obtained.

in a 0.1% bandwidth are generated per pulse in this energy range. By increasing the ruby laser energy from 1 J to 10 J, the number of photons generated per pulse increases by one order of magnitude. Ten Joule pulsed ruby lasers are well within the state of the art. Figure 13 shows that the conical angle of radiation increases rapidly at the lower beam energies if the bandwidth is constrained to be 0.1%. Because the total number of photons

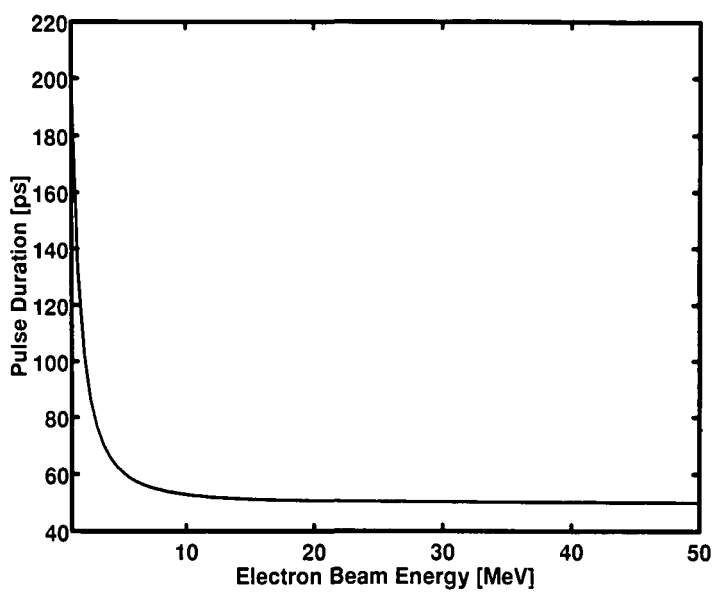

FIGURE 6. The pulse duration, as observed by a detector in the laboratory frame, is illustrated. The parameters of the interaction are stated in figure 4. For electron beam energies greater than about 5 MeV, the pulse duration is between 50 and 60 ps.

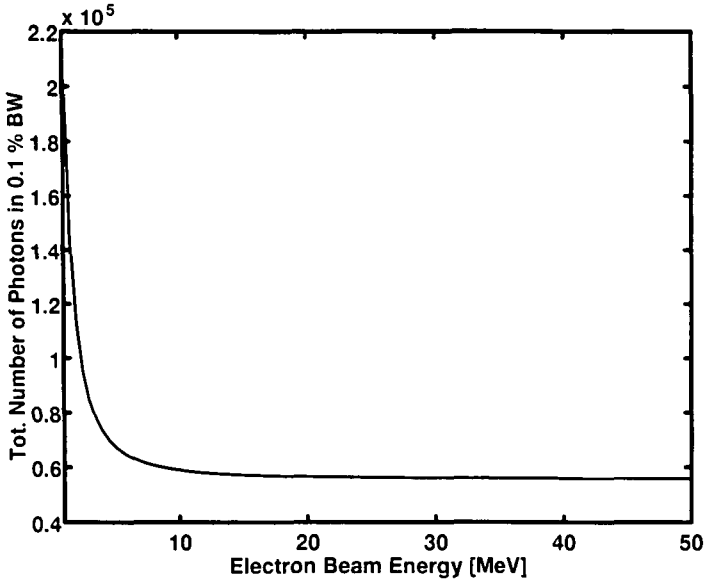

FIGURE 7. The total number of photons generated in a single pulse for the beam-beam parameters of figure 4 are shown. About a minimum of 6×10^4 photons are generated for beam energies between 5 to 50 MeV.

increases as the beam energy decreases (figure 12), a more selective bandwidth can be achieved by decreasing the aperture opening.

Although the number of scattered photons generated by the linear accelerator using inverse Compton scattering is about two to four orders of magnitude smaller than that of

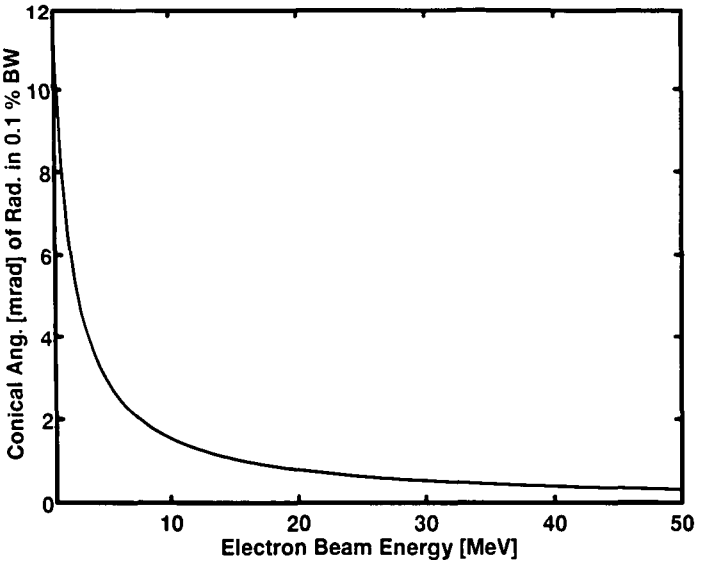

FIGURE 8. The conical angle subtended by the backscattered scattered radiation constrained within a 0.1% bandwidth is shown. For electron beam energies greater than about 5 MeV, the radiation is contained in a conical angle between 0 and 2 mrad. Near the 50-MeV electron range, the beam is about an order of magnitude narrower.

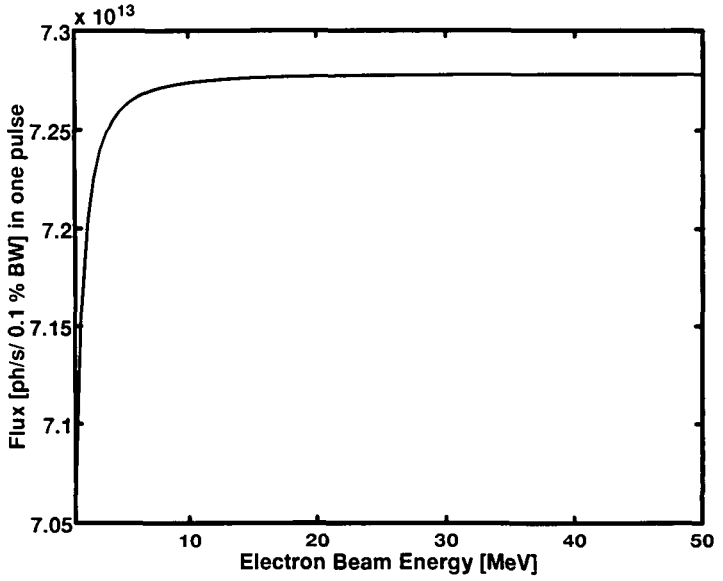

FIGURE 9. A 1-J, 5-ns pulsed, 1-mm waist, Gaussian ruby laser beam collides head-on with a 5-nC, 50-ps pulsed, 1-mm waist Gaussian electron beam with energies ranging between 1 and 50 MeV. The flux of photons in one pulse is depicted. For electron beam energies greater than about 5 MeV, the flux in a 0.1% bandwidth is relatively constant. The backscattered photon energies can be determined with the aid of figure 10.

the synchrotron sources, they are about an order of magnitude comparable at the experiment. Bragg diffraction gratings and X-ray mirrors are very lossy, especially in the soft X ray. It is not uncommon to have a diffraction grating or a monochromator efficiency between 1 and 10%. Further, the efficiency of X-ray mirrors is about 70%. Consequently,

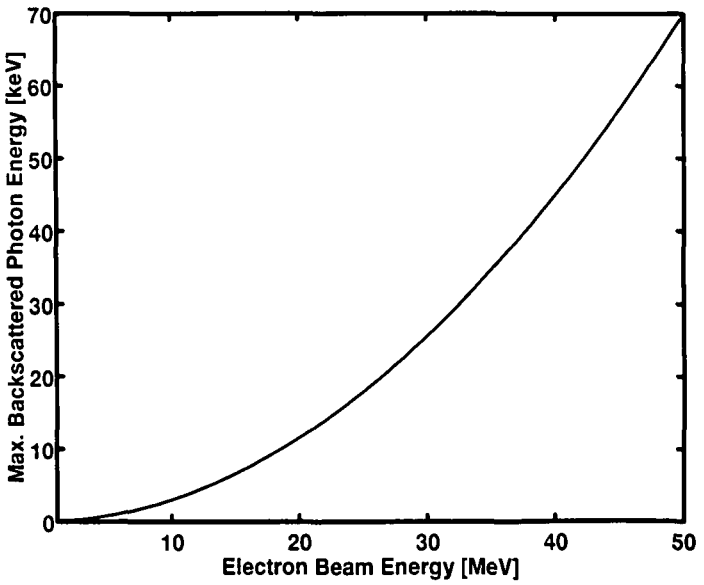

FIGURE 10. The backscattered photon energy ($\theta_o = 0$), resulting from a ruby photon colliding head-on with an electron, accelerated to energies between 1 and 50 MeV. Energies between 4.5 and 70 keV may be obtained.

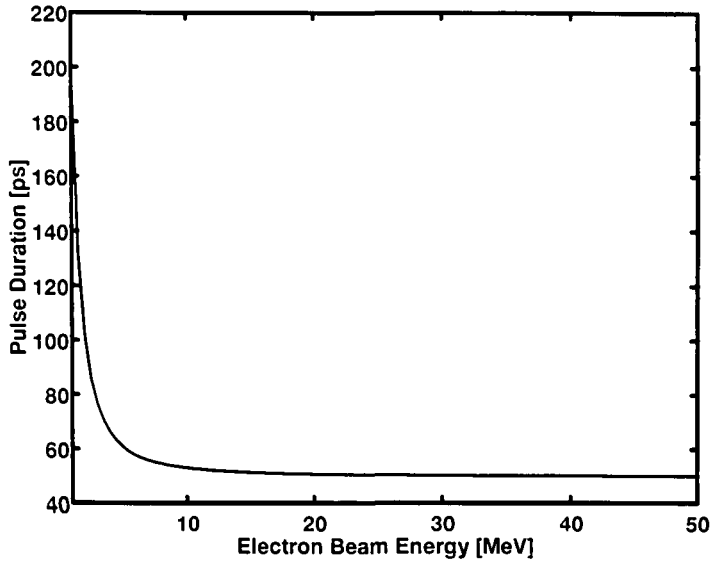

FIGURE 11. The pulse duration as observed by a detector in the laboratory frame is illustrated. The parameters of the interaction are stated in figure 9. For electron beam energies greater than about 5 MeV, the pulse duration is between 50 and 60 ps.

the number of photons reaching the experiment from a synchrotron source is about 1.5 to 2.5 orders of magnitude smaller than that generated in the machine. Because the Compton scattered photon energy is angle dependent, only a pinhole is required to block the undesired scattered radiation. Hence, the number of photons generated inside the interaction region of the linear accelerator equals that impinging on the experiment.

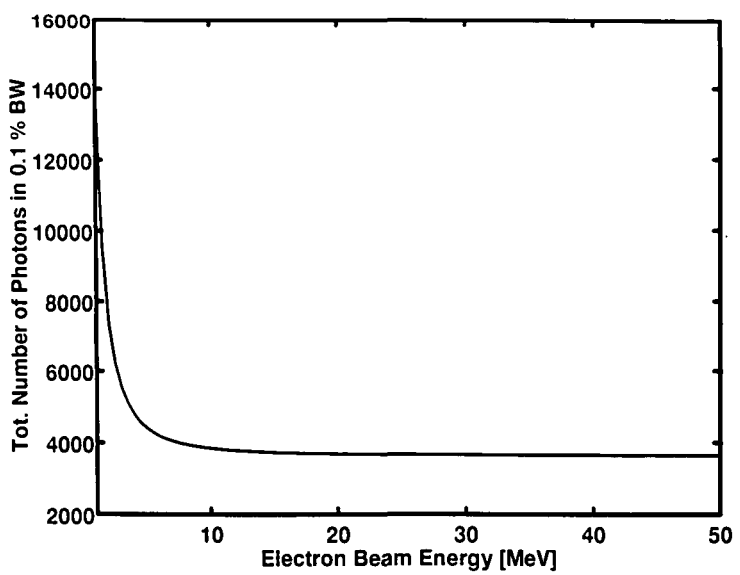

FIGURE 12. The total number of photons generated in a single pulse for the beam-beam parameters of figure 9 are shown. A minimum of about 3.75×10^3 photons in a 0.1% bandwidth is generated for beam energies between 5 to 50 MeV.

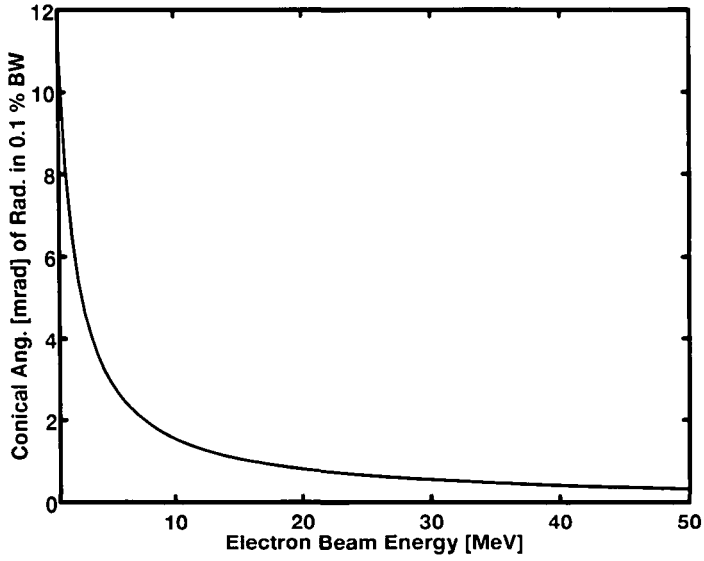

FIGURE 13. The conical angle subtended by the backscattered radiation constrained within a 0.1% bandwidth is shown. For electron beam energies greater than about 5 MeV, the radiation is contained in a conical angle between 0 and 2 mrad. Near the 50-MeV electron range, the beam is about an order of magnitude narrower.

The brilliance for the ALS (Lawrence Berkeley Laboratory Report 1994) and the APS (Shenoy *et al.* 1988; Lai *et al.* 1993) roughly does not exceed 3×10^{16} photons per second per mrad^2 per mm^2 in a 0.1% bandwidth *in either machine using wigglers.* The scattered energies of interest range from 0.1 keV to 100 keV. When a CO_2 laser beam is scattered, the brilliance, as shown in figures 5 and 14, ranges between 0.1 and 3.3×10^{21} pho-

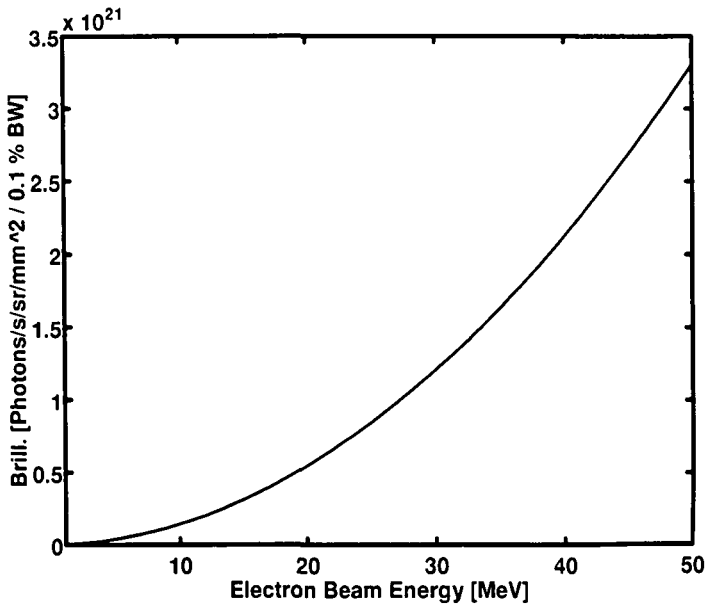

FIGURE 14. The brilliance resulting from the CO_2 laser scattering from the 1- to 50-MeV electron beam. Refer to the parameters given in figure 4.

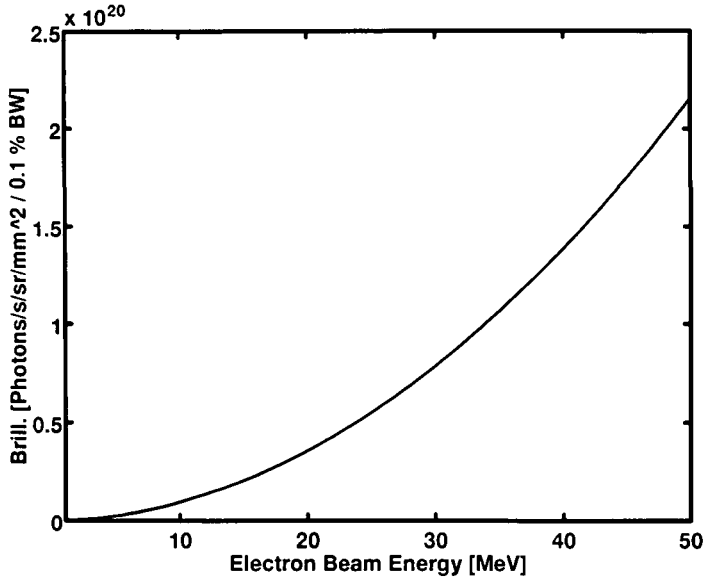

FIGURE 15. The brilliance resulting from the ruby laser scattering from the 1- to 50-MeV electron beam. Refer to the parameters given in figure 9.

tons/s/sr/mm^2 in a 0.1% bandwidth for scattered energies between 0.1 to 4.5 keV. For scattered energies between about 4 and 70 keV, the brilliance as observed in figures 9 and 15 ranges between 0.15 and 2.15 $\times$ 10^{20} photons/s/sr/mm^2 for a 0.1% bandwidth. This results from the scattering of the ruby laser beam. Note, the brilliance measure resulting from inverse Compton scattering *is at the experiment*. Decreasing these latter two numbers by about six orders of magnitude for the steradian units to be on the same order as the square of the mrad units, it is observed that the brilliance measure *at the experiment* is within one to three orders of magnitude compared to the brilliance *in* the synchrotron sources with wigglers.

Although the linear accelerator, as an X-ray light source, is approximately within a few orders of magnitude or exceeds in comparison to the synchrotron sources on a per-pulse basis, the ability to use this light source as a continuous source is beyond the state-of-the-art at present. Synchrotrons reuse the electron bunches for hours, whereas the electron bunch generated in the linear accelerator is used only once. Highly synchronous laser and accelerator pulses must be generated for the time duration of the experiment and must have a repetition frequency in the range of 5.6 to 381 MHz before they can be considered continuous relative to synchrotron sources. One means to reduce the stress on the cathode and reuse the spent electron beam is to circulate these electrons back into the accelerator. One design that accomplishes this is the race track microtron (Humphries 1986; Carroll 1990).

5. Applications

Various applications of a tunable VUV/X-ray source will be provided stressing commercial use. Low and medium energy accelerators with electron energies ranging from 0.12 to 16 MeV are commonplace in many disciplines. Medical centers use accelerators for cancer therapy and industry uses them for biomedical sterilization, curing of coatings and polymer crosslinking.

In the medical field, moderate energy linear accelerators 16 to 50 MeV coupled with a synchronous laser system using inverse Compton scattering can generate a highly tunable X-ray source over a broad bandwidth. The beam of X rays generated is narrow less than a 0.1° beamwidth. The soft and hard X rays penetrate the human tissue at different levels. Using the energy tunability properties of this light source along with possibly a chemical to capture the photon, one may be able to perform various surgical procedures internal to the body without the need for incisions. Due to the extreme narrow beam property, localized 3D surgery may be performed with minimal global tissue damage.

Spectroscopy is an important physical science that classifies and examines the chemical make-up of a substance. On an atomic level, the probability that a photon will interact with an atom is about 1% or less. Many photons are required in a continuous manner for appropriate analysis. If too many photons are generated at any one time, atomic and molecular interactions will result. This may be undesirable. A 0.1% bandwidth is typically needed for careful classification. The following is an example of a typical experiment. The estimated photon flux in the ALS machine is 2×10^{15} photons per second in the energy range of 500 eV to 2 keV. Losses resulting from 2 mirrors (70% efficiency) and 1 Bragg diffractor (1% efficiency) yields a photon flux at the experiment about 9.8×10^{12} photons per second. Due to recalibration limitations in the monitoring equipment, only two buckets positioned diametrically opposite to one another are used. Consequently, the calculated flux must decrease by a factor of 125. The number of photons per second at the experiment is 7.8×10^{10} photons per second with a pulse duration of 500 ps and a repetition rate of 3.2 MHz. If the present pulse repetition frequency of the linear accelerator can be increased to 1.2 kHz and a Diamond 84 CO_2 laser with a 450-mJ output energy and 1.2 kHz repetition frequency is used, the photon flux generated from Compton scattering is about 5×10^{14} photons per second. The pulse duration of the electron beam is typically 50 ps. As a result, the linear accelerator with inverse Compton scattering may play an important role in the field of spectroscopy. Further, it is conceivable to generate elliptically polarized X rays by appropriately polarizing the incident laser photon beam. This is useful in studying, for example, the dichroism effect.

Lithography requires large average powers, P_{ave}. Following the same line of reasoning from a different work (Sprangle *et al.* 1989), the exposure time to etch a 9-cm^2 wafer will be examined. The estimated chip exposure time for a cw source is

$$T_E = \frac{S}{P_{ave}} A_c$$

while that for a pulsed source is

$$T_E = \frac{S}{P_{peak}} \frac{T_{rep}}{T_p} A_c,$$

where S is the resist sensitivity, A_c is the area of the chip or wafer, P_{peak} is the peak power of the pulsed X-ray source, T_p is the pulse duration, T_{rep} is the pulse repetition period. High resolution resist such as polymethyl-methacrylate has a resist sensitivity of approximately 1 J/cm^2 at approximately 1 keV with a 0.1% bandwidth (Sprangle *et al.* 1989). Using the Diamond 84 laser (450 mJ at 1.2 kHz) and a 25-MeV, 5-nC, 50-ps electron beam, about 105 mW of X rays can be generated. The pulse duration is 50 ps with a repetition period of 833 μs. The exposure time needed to etch a 9 cm^2 wafer is about 1.4×10^9 s or about 4.5 years. Unless the resist sensitivity can be decreased by many orders of magnitude, this source is not practical for X-ray lithography.

For an X-ray microscope to be useful, it must be capable to produce images with an acceptable signal-to-noise ratio (SNR) in a reasonable amount of time. Consider the fol-

typical case (Buckley & Rarback 1990) and estimate the imaging time. The image is to have a 20% contrast and 256^2 pixels. For a SNR of 5:1, about 1000 transmitted photons per pixel are required on average. Consequently, about 7×10^7 photons are needed. A 1-J pulsed CO_2 laser with a repetition frequency of 180 Hz focused to a 1-mm waist collides head-on with a 25-MeV, 5-nC electron beam focused to a 1-mm waist to generate about 1.1×10^5 photons per second in a 50-ps pulse having a 0.1% bandwidth. Each pulse has enough photons for imaging a single pixel. The imaging time is limited solely by the repetition rate of the system. As a result, the imaging time is estimated to be about 364 seconds or 6.07 minutes. This is a reasonable time. The brilliance requirement (Buckley & Rarback 1990) for the beam must be at least on the order of 10^{12} photons per second per $mrad^2$ per mm^2 in a 0.1% bandwidth. This requirement is satisfied. Therefore, the linear accelerator with an appropriate laser source can be used for X-ray microscopy.

In some industries, detector calibration is a necessity for X-ray and VUV measurements. Some X-ray detectors, such as the windowless CsI detectors, have response curves in terms of power (EG&G Energy Measurements Inc. 1981). Here the response curve ranges between about 600 eV to about 2 or 3 keV. It will be assumed throughout this range that the detector response is about 10^3 A/MW. For 2-keV X rays generated in the ALS, the power per bunch has already been determined to be about 3.94 W. Optical and monochromator losses decrease the magnitude by about 2 orders of magnitude. The detector measures a power on the order of 39.4 mW, resulting in an output current of 39.4 μA. The voltage across a 50 Ω load is about 2 mV. The response is smaller for other X-ray beam energies: 0.5, 1, 10, and 20 keV. It appears that pulse mode calibration is possible for some beam energies but may be difficult for others. A 5-nC, 50-ps, 25-MeV electron beam colliding with a 1-J CO_2 laser beam both focused to a beam waist of 1 mm will generate over 0.2 W of 1.175 keV X rays (figures 5 and 16). Because only a pinhole is required to achieve a suitable bandwidth of 0.1%, this is the power at the detector. The CsI detector will generate

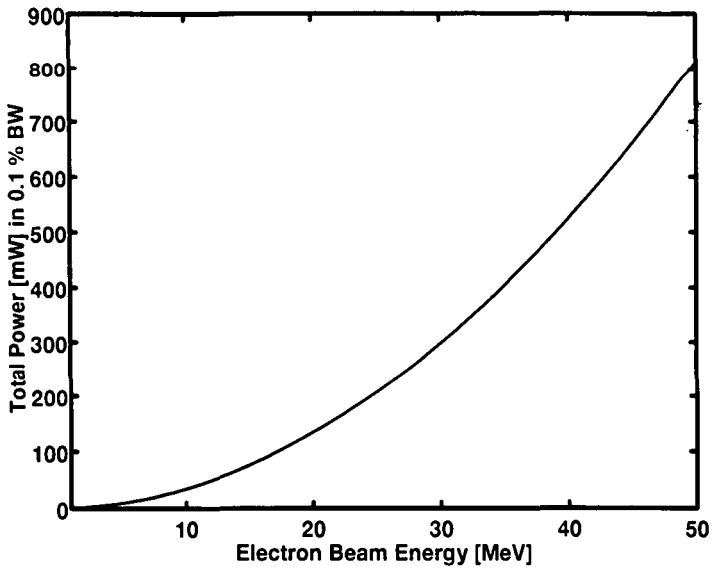

FIGURE 16. The total power scattered in a 0.1% bandwidth for a CO_2 laser colliding head-on with an electron beam with energies ranging between 1 and 50 MeV. The beam–beam characteristics are given in figure 4. With the aid of figure 5, a 25-MeV electron beam will generate about 0.2 W of 1.175-keV X rays.

about 0.2 mA of current or about 10 mV across a 50-Ω load. Pulse mode calibration appears as a promising application for this source.

6. Conclusion

A classical model characterizing the inverse Compton scattering mechanism between a pulsed electron linear accelerator and a pulsed laser has been used and compared to a quantum mechanical model. Good agreement has been shown thereby verifying the validity and correctness of the classical theory.

Comparisons between relatively new synchrotron accelerator sources (with insertion wiggler coils) and the rf electron linear accelerator source used as a VUV/X-ray source have been made. On a per-pulse basis, the 1- to 50-MeV linear accelerator has the capability of generating 0.1- to 70-keV X rays of substantial intensity comparable within a few orders of magnitude to the synchrotron accelerator with insertion coils at the experiment. For some energy ranges, the intensity exceeds that of the conventional synchrotron with wigglers. Even so, the state of the art has not advanced enough for practical continuous wave operation.

The various applications examined include X-ray spectroscopy, X-ray microscopy, and lithography. With existing industrial CO_2 lasers, it appears that a linear accelerator with a 1.2-kHz electron beam repetition rate can be used as a practical X-ray source in spectroscopy and microscopy. The repetition rates of both the laser and the electron beam source is three or more orders of magnitude too small to be a practical light source for lithography.

REFERENCES

Buckley, C.J. & Rarback, H. 1990 *Modern Microscopies Techniques and Applications*, P.J. Duke and A.G. Michette, eds. (Plenum Press, New York), p. 74.

Carroll, F. *et al.* 1990 *Invest. Radiol.* **25**, 465.

Carroll, F. 1991a *Lasers Surg. Med.* **11**, 72.

Carroll, F. 1991b In *Proc. of the International Conf. on Lasers*, p. 43.

Carroll, F. 1994 *J. X-Ray Sci. Techn.* **4**, 1.

Carroll, F. *et al.* 1994 *Invest. Radiol.* **29**, 266.

EG&G Energy Measurements Inc. 1981 *Los Alamos X-Ray Detector Calibration Sheet*, Detectors Division, Las Vegas Area Operations, Serial No. XRD-49-015-LV.

Esarey, E. *et al.* 1993 *Phys. Rev. E* **48**, 3003.

Humphries, Jr., S. 1986 *Principles of Charged Particle Acceleration* (John Wiley, New York), p. 493.

Jauch, J.M. & Rotrlich, F. 1995 *Theory of Photons and Electrons* (Addison Wesley, Reading, MA) p. 229.

Lai, B. *et al.* 1993 Argonne National Laboratory Report No. ANL/APS/TB-11.

Lawrence Berkeley Laboratory Report 1989 Report No. PUB 643 Rev. 2.

Lawrence Berkeley Laboratory Report 1994 Report No. LBL 35912 UC-411.

Silverman, J. 1995 In *IEEE Int. Conf. Plasma Sci.* (Madison, WI).

Schill, Jr., R.A. 1996 submitted for publ.

Shenoy, G.K. *et al.* Argonne National Lab. Report No. ANL-88-9.

Sprangle, P. *et al.* 1989 *Appl. Phys. Lett.* **55**, 2559.

Ting, A. *et al.* 1995 Naval Research Lab. Report No. NRL/MR/6790-95-7647.